An experiment to measure various diverse radioactive sources using a range of different detectors.

Jacob Gordon (201416406)

Department of Physics, The University of Liverpool.

20th of November 2021

Abstract:

Using a range of different detectors, various elements of radioactive isotopes were measured. The main method for experiments 1 and 2 required the use of Prospect to record the activity, energy, and time of different samples. The 3rd experiment involved the measurement of count rate/second against the thickness of Al sheets. All experiments were overall a success having the error fall within the accepted value for all but experiment 2. These results were 0.504 Bq/g/ci and 97.10$\pm$3.14 neutrons/cm^2/second for experiment 1. 3.66$\pm$0.034 minutes for experiment 2 and 1.78$\pm$0.577Mev for experiment 3.

1. Introduction

This report encompasses three separate experiments: measuring thermal neutron flux using active samples, determining the half-life of Vanadium 52, and finding the maximum electron energy's emitted by a Strontium 90 source. All these experimentations are focused on radiation detection. In 1909 Ernest B Rutherford's famous gold foil experiment proved the existence of the atomic nucleus by firing alpha particles at a thin gold foil. This important discovery could not have been made without the invention of the Giger counter by Rutherford's then lab assistant Hans Giger [1].

The device worked by applying a voltage between two electrodes, when applied any Alpha particles passing through the ionized gas would give of many electrons. Each particle passing would then be recorded by an electrometer [1]. The Geiger counter is still in use today although most often in an updated digital format. A Geiger counter was even used for experiment 3 as it was needed to measure the counts per second from our ^{90}Sr source. Over time more advanced detectors have been invented, the other two used in this experiment were a NaI scintillation detector and a High purity Germanium (HPGe) detector.

The main purpose of experiment 1 was to use both an Au water-moderated source and an Au carbon moderated source (measured in the NaI detector) to determine two values for the thermal neutron flux which would then be compared. The absolute neutron flux would be determined from an active ^{116}In sample (measured using the HPGe detector). Water and carbon moderators are most used in nuclear fission where they are used to slow neutron collisions [2]. For both the Au moderators and the ^{116}In each sample was placed in its respective detector and recorded for a time of 300 seconds.

Experiment 2 main purpose was to determine the half-life of ^{52}V, this was also done using the NaI detector. ^{52}V has a very short half-life so to effectively verify it the source was left in the detector for 1800 seconds. This way the full decay scheme was seen. Experiment 1 and 2 were recorded in Prospect.

Finally, experiment 3's purpose was to determine the maximum energy of electrons

emitted. A Giger counter was used to measure the range of electrons passing through Al sheets using the ^{90}Sr source. Counts per second were recorded as the thickness of Al was increased. A more detailed approach can be found in the Methodology.

2. Theory

The sources for Experiment 3 and 4 were made in a water tank. To produce these sources an americium-beryllium neutron source was used to produce high energy neutrons, these neutrons are the product of the reaction between the beryllium and the 5.5Mev alpha particles emitted by the americium. These alpha particles bombarded the source at a given distance of 10cm.

The reaction that produces these initial high energy neutrons is nuclear fission which through the process of neutron capture produces unstable nuclei. These neutrons then lose energy in the water tank. This process is called thermalisation as the neutrons approach the thermal energy of the water. The radioactive isotopes are then produced by neutron activation, where the neutrons are at low energies. They can be absorbed by atomic nuclei. These radioactive sources can decay via β particle and γ ray emission.

The neutrons in this reaction lose their energy in a water tank, this is known as a moderator. A moderator is any substance that slows down high velocity neutrons which increases the likelihood of nuclear fission [3]. The moderator used in the americium-beryllium reaction was water but other moderators such as graphite can be used. As mentioned before, the water moderator allows neutrons to reach their thermal energies. These energy's follow the Maxwell Boltzmann distribution with energy:

$$E = \frac{3}{2}k_B T$$

Equation 1 – Maxwell Boltzmann distribution

The energy of these thermal neutrons is 0.025ev. This is the energy corresponding to the most probable speed at a temperature of 290K, the mode of the maxwell Boltzmann distribution [4]. The ^{241}Am alpha particles produced have an initial activity of 0.5Ci and 3Ci for the water tank and graphite moderator respectively. As mentioned on the introduction both moderators will be investigated to determine which material is more effective at slowing down neutrons to their thermal energies.

Except for the ^{90}Sr experiment all data was recorded using the Prospect software. Counts were often measured against either energy (Kev) over a given time period or time itself. As a result, large data sets were produced that would be impractical to record without the aid of a computer. Prospect was used for both experiments 1 and 2. For experiment 1 the activity of the irradiated samples of Au in water and carbon needed to be determined as well as the activity of the ^{116}In. This was done using the equation for activity:

$$A_0 = \frac{\sigma m \eta \phi \alpha S}{w_A}$$

Equation 2 – Initial activity equation

It should be noted that A_0 is only the initial activity of the sample from when Prospect started recording data. It does not account for the time it took for the sample to reach the detector. To correct for this the following equation was used:

$$A = A_0 e^{-\lambda t}$$

Equation 3 – The decay in activity

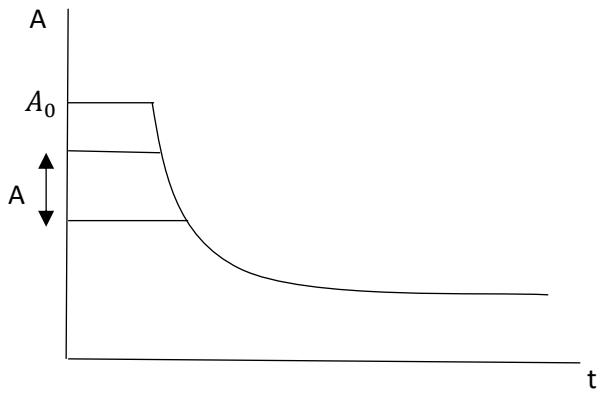

Figure 1 – A diagram to illustrate the change in activity over time.

Figure 1 demonstrates the change in activity over time. From the data only the activity of A could be found so equation 3 was used to correct for this. It should be known that the time for the sample to reach the detector was significantly shorter than for how long data was recorded for as figure 1 is not to scale.

The NaI detector was used to measure the counts from both the Au moderated sources and the ^{52}V source. This type of detector only identifies γ ray radiation and ignores alpha and beta radiation. When the radiation strikes the scintillator, it causes it to give off photons of visible light. These photons then strike a thin metal foil called a photocathode; light then enters the second part of the detector called the photo-multiplier tube (PMT). An electron is then ejected from the photocathode and a voltage accelerates it to a high energy where it knocks loose several other electrons [5]. From this the detector works out the energy and counts.

The HPGe detector was used to measure the ^{116}In. This detector works when ionizing radiation passes through the germanium crystal and interacts with the semiconductor material. Electron-hole pairs are produced when high energy photons pass through the detector ionize atoms of the semiconductor. As a result, a few electrons are then passed from the valence band to the conduction band. The germanium totally absorbs the high energy photons [6]. Under the influence of an electric field electrons and the holes travel to the electrodes and as a result a pulse is produced carrying all the information to Prospect.

The performance of these detectors can be measured using several metrics including, cost, energy resolution and most importantly efficiency. The absolute full energy peak is given by:

$$E_{abs} = \frac{I_\gamma}{A\Gamma t}$$

Equation 4 – Full energy peak efficiency.

This efficiency depends on several factors such as gamma ray energy and the distance from the source to the detector.

As mentioned in the introduction the purpose of the ^{90}Sr experiment is too find the maximum energy of electrons emitted. However, before that the electron range is needed.

$$R = 0.541E - 0.132$$

Equation 5 – 1 relation between electron range and energy.

$$R = 0.307E^{1.38}$$

Equation 6 - Another relation between electron range and energy

For electrons emitted with a continuous energy distribution, such as in β decay. Equations 5 and 6 are used to find the electron energy. All experiments performed in this block are counting experiments, meaning all measurements consist of counting how many times an event occurs over a given period. The uncertainty on all these experiments is the uncertainty on any count N which is $\sqrt{N}$.

3. Methodology

Experiment 1

To measure the relative thermal neutron flux of Au for both water and carbon moderated sources, the NaI scintillator detector was used.

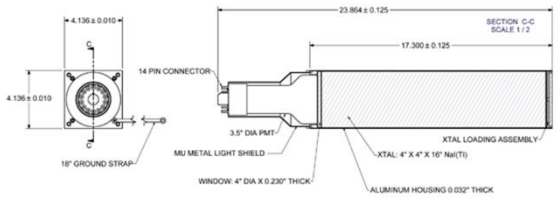

Figure 2 – A diagram of a NaI scintillator detector.

In figure 2 you can see an internal diagram of how the NaI detector works. Before readings could be taken the detector had to be calibrated. This was done using a ^{22}Na source. The source was placed in the detector for a pre-determined time of 300 seconds. 300 seconds was chosen to give the detector enough time to collect a reasonable amount of data. To keep things consistent 300 seconds was used as the time to collect all the data for this task.

After Prospect had collected all the data the ^{22}Na gave two peaks with energy peak around 510Kev and 1270Kev. The actual energy peaks are 511Kev and 1274.5Kev [7], this meant that the detectors were slightly out of phase so had to be corrected using the calibration setting on Prospect. To prove that the calibration was successful the experiment was repeated with ^{88}Y. The energy's found from this calibration were 898.0Kev and 1836.1Kev which is the same as the known values [8] showing that the calibration was successful. Both ^{22}Na and ^{88}Y were good sources to calibrate with. This is because both only have two distinct energy peaks which were far away from each other. This meant it was easy to distinguish between the peaks and compare them to the known values (All calibration data can find in Appendix B).

Before the experiment began the Au sources were weighted. The Au water source was 6.9 ± 0.1g and the carbon source was 3.9 ± 0.1g, this would be needed for analysis later. Firstly, the Au in water source was placed in the detector and the counts were recorded for 300 seconds. The same process was then repeated for the graphite moderated source.

The second part of experiment 1 was to measure the neutron flux of the active ^{116}In sample. This was done using the HPGe detector.

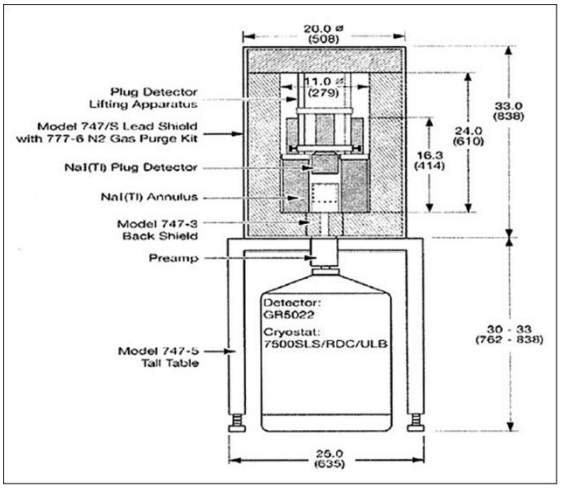

Figure 3 – A diagram of a HPGe detector.

Figure 3 shows a diagram of the setup used for this part of the task. This detector also had to be calibrated before measurements could be taken, this was done using a ^{152}Eu source. The source was placed inside the detector upright and data was taken for 300 seconds. Prospect then produced 6 different peaks relating to the ^{152}Eu energies. These energies were then recorded and compared to the known values [9]. Prospects calibration feature was then used to correct to the actual ^{152}Eu values.

Once this was done the same process was repeated for ^{116}In to obtain its energy values. It should be noted that both the ^{152}Eu and the ^{116}In source were in a container of the same dimensions. This is important as the same proportions were needed to keep the experiment consistent and they would also be needed in the LABSOC modelling software. The dimensions are as follows:

Dimension	Value (cm)	Material
Wall thickness	0.16 ± 0.1	Polypropylene
Side walls	1.7 ± 0.1	Polypropylene
Bottom walls	1.7 ± 0.1	Polypropylene
Source	2.2 ± 0.1	Sand
Absorber	2.2 ± 0.1	Epoxy
Source detector	2.3 ± 0.1	N/A

Table 1 – Dimensions inputted into LABSOC.

LABSOC was software we used to model the efficiency of the ^{152}Eu and ^{116}In sources, table 1 shows the dimensions of the samples inputted into this software. The energy peaks of both sources were also entered. The efficiencies were then plotted against the energies to generate an efficiency curve. This was needed as these values were needed to work out the activity, this can be seen in equation 4.

Experiment 2

To measure the ^{52}V the NaI detector was set up slightly different than in experiment 1. Instead of measuring counts against energy counts against time was recorded. The dwell time on Prospect was set to 10 seconds, this meant prospect only recoded data every 10 seconds. This was because ^{52}V decayed incredible quicky so by setting the dwell time to 10 seconds and recording data over a long period of time (1800 seconds) the full decay of ^{52}V could be seen. To record counts against time Prospect was set in "MCS" mode.

Experiment 3

For this task counts per second were measured against Al thickness.

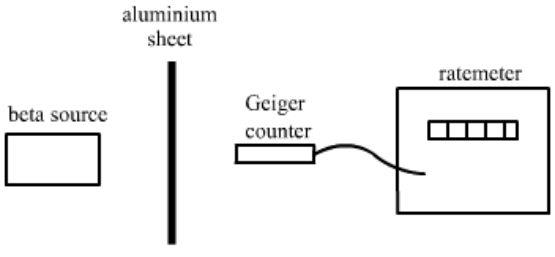

Figure 4 – A simplified setup of task 5.

In figure 4 the beta source was the ^{90}Sr source, as it is a pure β emitter Al sheets will stop any radiation passing through. The thickness of the Al sheets was increased and counts per second were recorded with each increase in thickness. Every measurement was recorded for 60 seconds. This was to make it easier to see the change in counts per second as at high time and low thickness the counts often went past the maximum resolution of the Geiger counter. When measuring the thickness of the Al a micrometre was used, the thickness of the Al was measured at the bottom, middle and top of the sheet and an average was taken.

The thickness of the Al sheets was going to be increased in 0.2mm increments until 20 values were recorded. However, the thickness was not always even. This led to an approximation of 0.2mm. For example, instead of 0.2mm 0.195mm was used as our first value and 0.446mm for our second value. 20 values were still recorded for this increase. From these values a value of the electron range could be determined and in turn a value for the maximum energy of the electrons.

4. Results and Analysis

Experiment 1

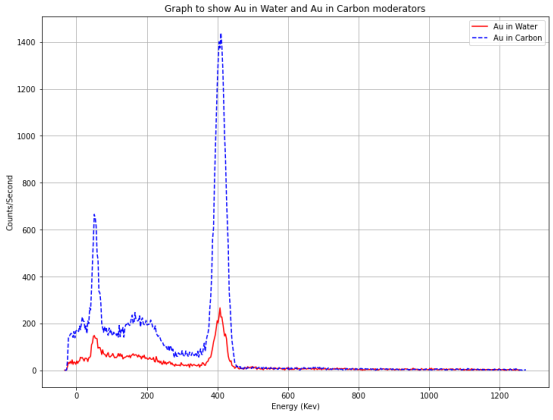

Figure 5 – Graph to shown Counts vs time for an Au water and carbon moderator.

From figure 5 it can be observed that both sources follow a similar distribution. However, the energy peaks for Au moderated in carbon is much greater than that of water, specifically the main peak at 400Kev. This means that at

the same energy, a much greater number of neutrons were detected.

To determine which moderator was better a relative value of the thermal neutron flux was obtained using the following equation:

$$\frac{water}{carbon} = 6\frac{water_{cps}m_C}{carbon_{cps}m_W}$$

Equation 7 – ratio of water moderator over carbon

Using equation 7 a ratio of the water moderator over the carbon could be found, this was done as only a relative value of neutron flux was needed to determine the better moderator. The value obtained from this equation was 0.504 Bq/g/ci, This positive value shows that carbon is a better moderator than water.

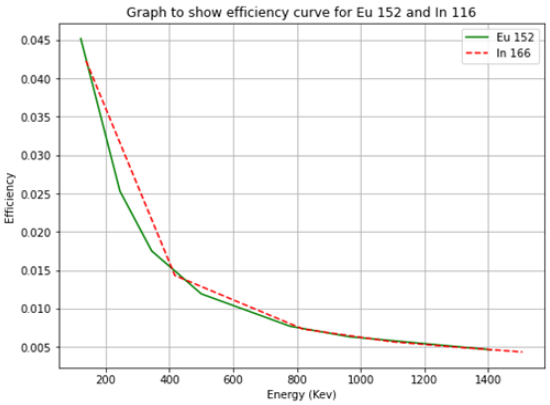

Figure 6 – A graph to show the efficiency curves for ^{152}Eu and ^{116}In.

The general trend shown in figure 6 is that as the energy increases the efficiency decreases. As ^{152}Eu was used for calibration its efficiency curve is only a model. The values for ^{116}In were experimental values, the aim was to try and get the ^{116}In as close as possible to the ^{152}Eu model. As you can see from the figure both curves are very similar, especially at high energies (above 800Kev) where both curves matched up perfectly. This is not true for lower energies (below 800Kev). This is because at low energy the efficiency varies by a greater degree. Overall, the ^{116}In data is a good fit for the model.

Once efficiency values had been obtained, the values for activity were calcualted

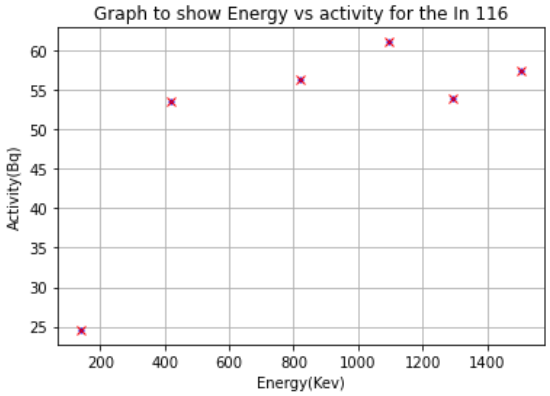

Figure 7 – Activity vs energy for a ^{116}In source.

The general trend in figure 7 is that as energy increases the activity stays consistent. To arrive at values for activity the efficiency values from our ^{116}In were used in conjunction with equation 4 to generate an array of activity values. Looking at figure 7 the first data point is an obvious outlier; this is because at low energy the efficiency curve is very sensitive as the ^{116}In begin to absorb back into itself causing low energy data to be skewed. This also explains the low energy discrepancies in figure 6.

The error on the activity was worked out using the following equations:

$$A_{err} = \sqrt{(\frac{\Gamma t_{err}}{\Gamma t})^2 + (\frac{I_{\gamma err}}{I_\gamma})^2}$$

Equation 8 – The error on the activity.

Equation 8 was used to work out the errors on the calculated activity (full derivation in Appendix A). The first error was the error on both the gamma fraction and time combined, the second error was on number of counts in a full energy peak (This was the net area of the peak on prospect).

To calculate a final activity value the weighted mean on the activity was taken, this was done as the data points varied by a reasonable amount (full calculation in Appendix B). The final value for the activity was $55.98 \pm$

$0.014\ Bq$. It should be noted that this is not the initial value of the sample but only the activity value from when data started to be taken.

Using equations 2 and 3 a value of the thermal neutron flux could be calculated. This value was 97.10±3.14 neutrons/cm^2/second. This is within the expected range of values of between 10 and 100 neutrons/cm^2/second. To calculate the error on this value the following equation was used:

$$\phi_{err} = \sqrt{(\frac{A_{0err}}{A_0})^2 + (\frac{m_{err}}{m})^2 + (\frac{\sigma_{err}}{\sigma})^2}$$

Equation 9 – The error on the thermal neutron flux.

The first error is that on the activity calculated in equation 8, the second error is the standard error on the mass of ^{116}In and the final error was the error on the neutron capture cross section.

Experiment 2

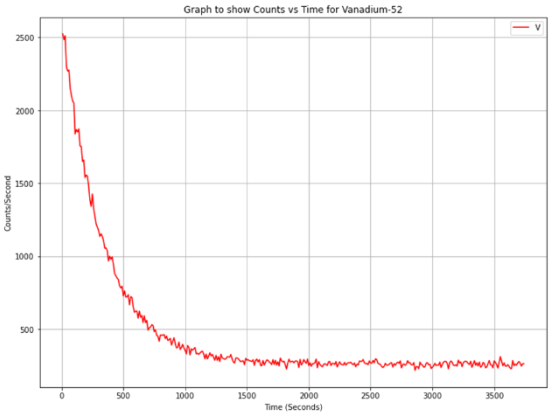

Figure 8 – Graph to show count rate vs time for ^{52}V.

The general trend for figure 8 is that as time increases the count rate decreases. It is known that the half-life of ^{52}V is very short, this explains the long tail at the end of the graph past 800 seconds. Before this value is the decay of the ^{52}V whereas after the graph tails of into just background readings.

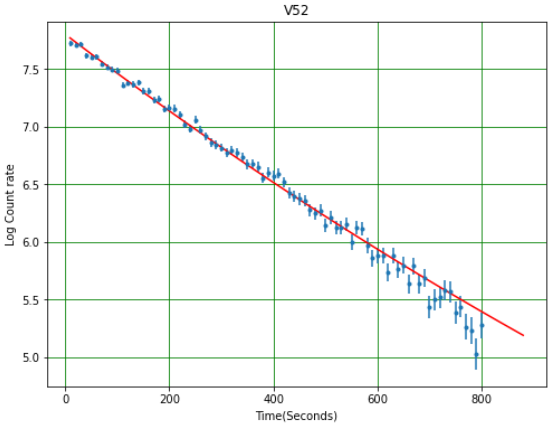

Figure 9 – Graph to show Log count rate vs time for ^{52}V.

The general trend for figure 9 is a negative linear gradient. Figure 9 is the log graph of figure 8 not including the background readings, hence why it ends at 800 seconds. The negative gradient from this graph was -0.00316, this value is the decay constant of ^{52}V. To find a value for the half life the following equation was used:

$$T_{1/2} = \frac{\ln(2)}{\lambda}$$

Equation 10 – The half-life equation.

From this a value of 219.65 seconds was found, converting to minutes this becomes 3.66±0.034 minutes. The known value of the half-life is 3.74 minutes [10]. Although the known value is technically outside the range of the calculated error our value is only 0.1 minutes off leading to the conclusion that the experiment was a success but with a small error.

The reason why the error is so small is because it is the standard error taken on the decay constant (gradient). Since this number was so small the standard error was even smaller. The error on the data points for time

in figure 9 was the standard error on time of 0.01 seconds. The error on the counts was calculated as follows:

$$N_{err} = \frac{\sqrt{(N_{berr})^2 + (\sqrt{N})^2}}{N_b}$$

Equation 11 – The error on counts

The background count and its error were calculated by taking the mean of all the background values (Past 800 seconds) and for the error square rooting this value. The chi squared value for figure 9 was 1.40, this shows that the line of best fit was a good approximation for the data as the expected results fit the observed results.

Experiment 3

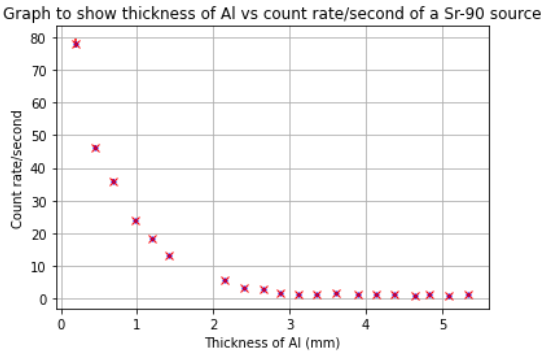

Figure 10 – A graph of count rate/second vs thickness for a ^{90}Sr source.

The general trend from figure 10 is that as Thickness increases the count rate/ second decreases. It can be seen in the figure that the negative distribution hits a point where it no longer decreases. This is when the Al has become so thick that the β particles can no longer penetrate it and the Geiger counter only detects background radiation.

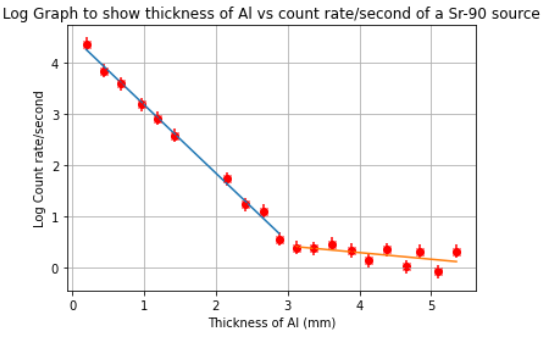

Figure 11 – A log graph of count rate/second vs thickness of Al for a ^{90}Sr source.

In figure 11 you can see more clearly where the count rate begins to only detect background. To calculate the error on the thickness the standard deviation was used as 3 values for thickness were recorded. To Calculate the error on the Count rate the following equation was used:

$$N_{final\ err} = \sqrt{(N_{err})^2 + (N_{berr})^2}$$

Equation 12 – The final count rate error

The intersection of the ^{90}Sr decay gradient and the background gradient will give us a value for the electron range.

$$R = \frac{1}{m_2 - m_1}(N_2 - N_1)$$

Equation 13 – The simultaneous equation used to find the electron range

By solving using simultaneous equations the calculated value of electron range was 3.059 ± 0.325cm. To calculate the error on R the differential of equation 13 needed to be taken:

$$R_{err} = \sqrt{(\frac{dR}{dm_{err}})^2 + (\frac{dR}{dN_{err}})^2}$$

Equation 14 – The error on the electron range.

The final step was the calculate the value for the maximum energy of electrons emitted. Using the value for R in combination with equations 5 and 6 two values were obtained. These values were 1.78Mev and 1.67Mev. However, as equation 6 only allows values between 0.15Mev and 0.8Mev the second value was disregarded. Therefore, the final value was 1.78 ± 0.577Mev. This may seem far off the known ^{90}Sr energy value of 0.546Mev [11] however ^{90}Sr decays into ^{90}Ymeaning the energy value that should be compared to is 2.28Mev [12]. This puts the accepted value within the error of the calculated value. To find the final error the error on R was multiplied by our value for the energy.

5. Discussion

Experiment 1

The relative thermal neutron flux obtain was 0.504 Bq/g/ci. For the gold moderated source, a ratio of the flux of water over carbon was taken instead of absolute values, this is because a relative value more clearly shows which moderator was more effective, in this experiment it was the carbon. This is because water moderators have a high neutron capture cross section because of its inability to form deuterium molecules. This means that water can only be used as a moderator with enriched fuels. Graphite moderators have a lower neutron cross section and are more thermally stable [13].

The calculated absolute value for thermal neutron flux was within the accepted range of the known value overall making this experiment a success. There were a lot of errors that had to be accounted for when calculating this final value, some of which were given errors (such as the gamma fraction) while others had to be determined during the experiment. The two most notable errors were that on the mass and on the activity, the error on the activity came from $I_\gamma$and the time. To improve the error on the mass more accurate weighing scales could have been used with a greater resolution. To improve the error on the activity the data could have been taken for a greater period, also the time it took to move the source from the water tank to the detector could have been recorded and factored into the error. This would have also given a more accurate final value.

Experiment 2

This experiment was also a success, even though the calculated value of 3.66 ± 0.034 minutes error did not encompass the actual value of 3.74 minutes this was only due to a small error. The known value is less than 0.1 minutes away meaning the two values are very close. The reason for this incredibly small error is because the decay constant error (gradient error) was used and as the decay constant was so small this led to an even smaller error. This would not have been an issue with an element with a longer half-life.

To improve this error a more accurate gradient would need to be taken, this could be done be capping the time value to a lower number to make sure no background readings are being considered.

Experiment 3

The final value of 1.78 ± 0.577Mev error lied within the known value of 2.28Mev making this experiment overall a success. The main errors in this experiment were that on the thickness of Al and the count rate/ second. The thickness error could have been improved by taking more readings of the Al at different areas around the Al sheet and with equipment of a greater resolution than a micrometre. To improve the count rate error each measurement could have run for longer than 60 seconds, however this would require a Geiger counter with a higher resolution.

One discrepancy that affected the results in this experiment was the thickness of the Al sheets. Each sheet was a minimum thickness of roughly 0.2mm, this limited the number of readings that could be taken before the Geiger counter began to pick up only background radiation. This could have led to a less accurate gradient on figure 11.

Overall, if this experiment were to be repeated it could be improved by using more accurate detectors, specifically for experiment 1 and 2. The HPGe detector gave incredibly accurate readings for the ^{152}Eu and ^{116}In, in these experiments' limits were placed on what the HPGe detector could be used to measure but if this detector was used to measure the Au and ^{52}V more accurate values for the peaks would have been obtained.

6. Conclusion

To conclude, various radiation detectors were used to measure activity and energy from many different radioactive isotopes. The experiments were performed by placing each source in its assigned detector and taking measurements with the Prospect software. Except for ^{90}Sr where the thickness of Al was changed.

All results for these 3 experiments errors lay either within or extremely close to the known values making every experiment a success. If the experiments were to be repeated using the HPGe detector for both the Au and ^{52}V would yield more accurate energy values and lower thickness Al sheets would lead to a more accurate electron range.

7. References

[1] - Aps.org. 2021. *June 1911: Invention of the Geiger Counter*. [online] Available at: <https://www.aps.org/publications/apsnews/201206/physicshistory.cfm> [Accessed 21 November 2021].

[2] - Hyperphysics.phy-astr.gsu.edu. 2021. *The Moderation of Fission Reactions*. [online] Available at: <http://hyperphysics.phy-astr.gsu.edu/hbase/NucEne/moder.html#:~:text=Water%20and%20carbon%20(graphite)%20are,Canadian%20reactors%2C%20avoids%20this%20loss> [Accessed 21 November 2021].

[3] - NRC Web. 2021. *Moderator*. [online] Available at: <https://www.nrc.gov/reading-rm/basic-ref/glossary/moderator.html> [Accessed 21 November 2021].

[4] - Nuclear Power. 2021. *Neutron Energy | Classification of Neutrons | nuclear-power.com*. [online] Available at: <https://www.nuclear-power.com/nuclear-power/reactor-physics/atomic-nuclear-physics/fundamental-particles/neutron/neutron-energy/> [Accessed 21 November 2021].

[5] - Nevada Technical Associates, Inc. 2021. *How Do Sodium Iodide (Scintillation) Detectors Work?*. [online] Available at: <https://www.ntanet.net/how-do-sodium-iodide-scintillation-detectors-work> [Accessed 21 November 2021].

[6] - Nuclear Power. 2021. *Principle of Operation of HPGe Detectors | nuclear-power.com*. [online] Available at: <https://www.nuclear-power.com/nuclear-engineering/radiation-detection/semiconductor-detectors/high-purity-germanium-detectors-hpge/principle-of-operation-of-hpge-detectors/> [Accessed 21 November 2021].

[7] - Nucleardata.nuclear.lu.se. 2021. *Table of Isotopes decay data*. [online] Available at: <http://nucleardata.nuclear.lu.se/toi/nuclide.asp?iZA=110022> [Accessed 21 November 2021].

[8] - Nucleardata.nuclear.lu.se. 2021. *Table of Isotopes decay data*. [online] Available at: <http://nucleardata.nuclear.lu.se/toi/nuclide.asp?iZA=390088> [Accessed 21 November 2021].

[9] - Nucleardata.nuclear.lu.se. 2021. *Table of Isotopes decay data*. [online] Available at: <http://nucleardata.nuclear.lu.se/toi/nuclide.asp?iZA=630152> [Accessed 21 November 2021].

[10] - Education.jlab.org. 2021. *It's Elemental - The Element Vanadium*. [online] Available at: <https://education.jlab.org/itselemental/iso023.html> [Accessed 21 November 2021].

[11] - Nucleardata.nuclear.lu.se. 2021. *Table of Isotopes decay data*. [online] Available at: <http://nucleardata.nuclear.lu.se/toi/nuclide.asp?iZA=380090> [Accessed 21 November 2021].

[12] - Nucleardata.nuclear.lu.se. 2021. *Table of Isotopes decay data*. [online] Available at: <http://nucleardata.nuclear.lu.se/toi/nuclide.asp?iZA=390090> [Accessed 21 November 2021].

[13] - Energyeducation.ca. 2021. *Neutron moderator - Energy Education*. [online] Available at: <https://energyeducation.ca/encyclopedia/Neutron_moderator> [Accessed 21 November 2021].

8. Appendix A – Error calculation.

Experiment 1

Error on activity:

$$\Gamma t_{err} = \sqrt{(\frac{\Gamma_{err}}{\Gamma})^2 + (\frac{t_{err}}{t})^2}$$

$$A_{err} = \sqrt{(\frac{\Gamma t_{err}}{\Gamma t})^2 + (\frac{I_{\gamma err}}{I_\gamma})^2}$$

Weighted mean (On activity):

$$W = (\frac{1}{A_{err}})^2$$

$$A_{0top} = \sum A_0 W$$

$$A_{0bottom} = \sum W$$

$$W_{err} = \sqrt{\frac{1}{\sum W}}$$

$$A_{0W} = \frac{A_{0top}}{A_{0bottom}}$$

Error on neutron flux:

$$\phi_{err} = \sqrt{(\frac{A_{0err}}{A_0})^2 + (\frac{m_{err}}{m})^2 + (\frac{\sigma_{err}}{\sigma})^2}$$

Experiment 2

Error on counts:

$$N_{err} = \sqrt{N}$$

$$N_{final} = N - N_b$$

$$N_{err} = \frac{\sqrt{(N_{berr})^2 + (\sqrt{N})^2}}{N_b}$$

Error on half-life (minutes):

$$T_{1/2err} = \frac{\lambda_{err}}{\lambda}\frac{T_{1/2}}{60}$$

Experiment 3

Error on Counts:

$$N_{berr} = \sqrt{N_b}$$

$$N_{err} = \sqrt{\frac{N^2}{t^2} + \frac{{t_{err}}^2}{t^4}}$$

$$N_{berr} = \sqrt{\frac{{N_b}^2}{t^2} + \frac{{t_{err}}^2}{t^4}}$$

$$N_{err\ final} = N_{err} + N_{berr}$$

Error on Log of counts:

$$\ln{(N_{err\ final})_{err}} = \ln{(\frac{N_{err\ final}}{N})}$$

Error on electron range:

$$m = m_2 - m_1$$

$$N = N_2 - N_1$$

$$m_{err} = \sqrt{{m_{1err}}^2 + {m_{2err}}^2}$$

$$N_{err} = \sqrt{{N_{1err}}^2 + {N_{2err}}^2}$$

$$\frac{dR}{dm_{err}} = N ln(m_{err}) m_{err}$$

$$\frac{dR}{dN_{err}} = \frac{1}{m_{err}} N_{err}$$

$$R_{err} = \sqrt{(\frac{dR}{dm_{err}})^2 + (\frac{dR}{dN_{err}})^2}$$

Error on Max energy emitted:

$$E_{err} = E R_{err}$$

8. Appendix B – Other relevant information.

Calibration data:

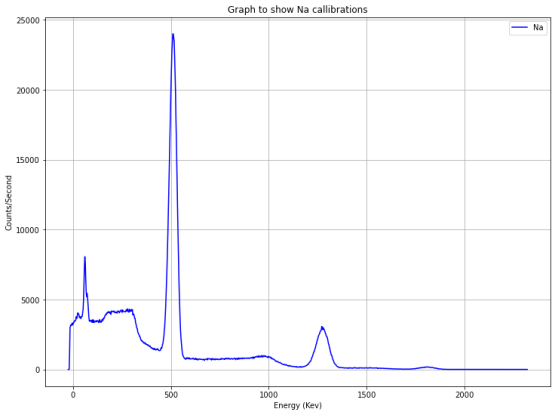

Figure 12 – Na calibration

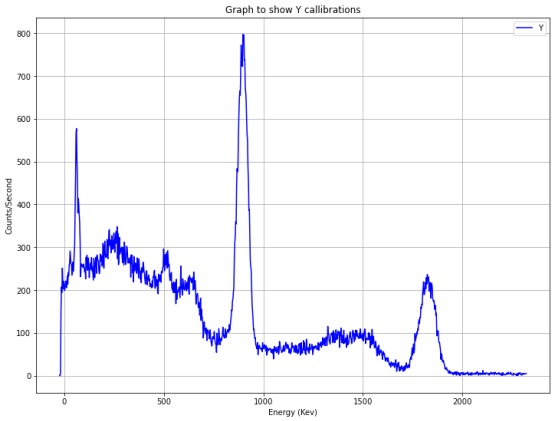

Figure 13 – Y calibration data

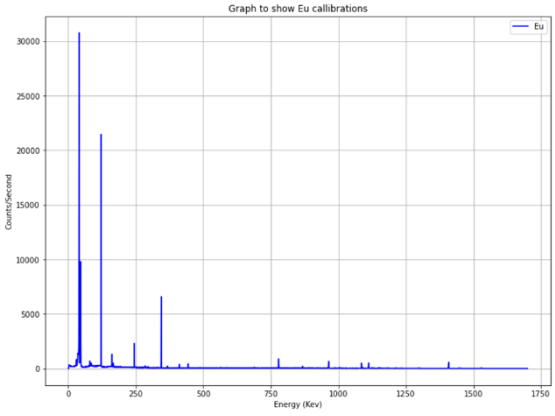

Figure 14 – Eu calibration data

Tables of raw data:

Experiment 1:

^{152}Eu energy (Kev)	^{152}Eu efficiency (arb)
121.8	4.52e-02
244.7	2.53e-02
344.3	1.75e-02
500.0	1.19e-02
778.9	7.63e-03
964.1	6.31e-03
1408.1	4.61e-03

Table 2 – Energy and efficiency value for ^{152}Eu

^{116}In energy (Kev)	^{116}In efficiency (arb)
138.4	4.23e-02
417.0	1.43e-02
818.7	7.31e-03
1097.2	5.66e-03
1293.5	4.97e-03
1507.5	4.32e-03

Table 3 – Energy and efficiency values for ^{116}In

Γ (Gamma ray/decay)	ΔΓ (Gamma ray/decay)
3.90	0.14
32.8	0.14
13.6	0.5
66.6	0.13
100.2	0.2
11.8	0.4

Table 4 – Gamma fractions and their errors

I_γ(Num. of counts)	ΔI_γ(Num. of counts)
1216.57	325.47
7532.0	157.51
1682.27	126.79
6909.68	163.76
8067.68	129.7
879.73	63.24

Table 5 – Number of counts In full energy peak with error

Activity (Bq)	ΔActivity (Bq)
24.58	2.77
53.53	0.044
56.41	0.81
61.10	0.025
54.00	0.017
57.53	0.86

Table 6 – Activity and their errors.

Experiment 3

N (Counts/second)	ΔN(Counts/second)
78.21	1.30
46.21	0.77
35.91	0.59
24.09	0.40
18.28	0.30
13.18	0.22
5.66	0.094
3.41	0.057
3.01	0.050
1.74	0.029
1.46	0.025
1.44	0.025
1.58	0.027
1.39	0.024
1.14	0.020
1.41	0.024
1.01	0.018
1.36	0.023
0.92	0.017
1.36	0.023

Table 7 – Count rate and its errors for experiment 3

Thickness of Al (mm)	ΔThickness on Al (mm)
0.195	0.00408
0.446	0.00235
0.685	0.00408
0.970	0.0047
1.19	0.0047
1.42	0.0164
2.15	0.00236
2.41	0.0165
2.66	0.00816
2.88	0.026
3.12	0.00417
3.36	0.00236
3.61	0.012
3.89	0.000471
4.13	0.0047
4.38	0.00471
4.65	0.028
4.83	0.00707
5.09	0.00471
5.35	0.012

Table 8 – Thickness of Al and its errors for experiment 3